Studies on the redox behaviour of $La_{1.867}Th_{0.100}CuO_4$ and its catalytic performance for NO decomposition

Gao, L. Z.; Au, C. T.

Published in:
Catalysis Letters

DOI:
10.1023/a:1019077507513

Published: 01/03/2000

Document Version:
Early version, also known as preprint

Studies on the redox behaviour of $La_{1.867}Th_{0.1}CuO_4$ and its catalytic performance for NO decomposition

L.Z. Gao[†] and C.T. Au[*]

Chemistry Department and Center for Surface Analysis and Research,

Hong Kong Baptist University, Kowloon Tong, Kowloon, Hong Kong, China

Dr. Peter C.T. Au, CCHEM, FRSC

Chemistry Department and

Center for Surface Analysis and Research,

Hong Kong Baptist University,

Kowloon Tong, Kowloon,

Hong Kong

Tel: (852) 2339 7067

Fax: (852) 2339 7348

E-mail: pctau@hkbu.edu.hk

* To whom correspondence should be addressed

† Present address: Chengdu Institute of Organic Chemistry, Chinese Academy of Sciences, Chengdu 610041, P.R. China

Studies on the redox behaviour of $La_{1.867}Th_{0.1}CuO_4$ and its catalytic performance for NO decomposition

L.Z. Gao[†] and C.T. Au[*]

Department of Chemistry and Center for Surface Analysis and Research, Hong Kong Baptist University, Kowloon Tong, Kowloon, Hong Kong, China.

$La_{1.867}Th_{0.1}CuO_4$ was prepared by means of the citric acid complexing method. The reduction-oxidation (redox) properties of this composite oxide have been investigated by means of the *in situ* XRD, TGA, EPR, and TPD methods. The fresh (non-reduced) $La_{1.867}Th_{0.1}CuO_4$ catalyst is single phase with tetragonal K_2NiF_4-type structure. There were three reduction steps observed over $La_{1.867}Th_{0.1}CuO_4$ in the temperature ranges of 25-100°C, 100-300°C, and 300-500°C, respectively. At 300°C, the material still retained its original single phase but there were oxygen vacancies generated in the lattice. At 500°C, it decomposed to a mixture of oxides. In the course of reduction, trapped electrons were generated. During the oxidation of the reduced sample, O_2^- was detected. Apparently, oxygen vacancies are able to stabilize O_2^- on the surface of the catalyst. NO adsorption on both fresh and reduced $La_{1.867}Th_{0.1}CuO_4$ samples generated NO^- species which decomposed to N_2O and O_2^-. The decomposition of N_2O would result in N_2 and O_2 generation. On a $La_{1.867}Th_{0.1}CuO_4$ sample reduced at 300°C, NO_2^- coupled with O_2^- to form the intermediate $[O_2NO_2]^{2-}$

which decomposed to N_2 and O^{2-}. After reduction, the O^{2-} inside the lattice became more mobile and participated in the $[O_2NO_2]^{2-}$ decomposition process.

Keywords: $La_{1.867}Th_{0.1}CuO_4$, redox behaviour, NO decomposition

† Present address: Chengdu Institute of Organic Chemistry, Chinese Academy of Sciences, Chengdu, 610041, P.R.China.

* Corresponding author

1. Introduction

Perovskite type (ABO_3) mixed oxides are known to be active catalysts for NO_x reduction and ammonia oxidation [1, 2]. They are thermally stable (up to 1000°C) and can accommodate lattice defects such as oxygen vacancies, *A*-site deficiencies, and *B* ion of variable oxidation states. The perovskite-like A_2BO_4 mixed oxides of K_2NiF_4 structure are thermally more stable than ABO_3 and have been described as novel catalysts for ammonia oxidation and NO_x elimination [3-5]. In general, in ABO_3 and A_2BO_4, *A* is a rare earth element and *B* is a transition metal; the oxidation state of *B* is +2 and +3, respectively, in the two compounds. Besides noble metals such as Pt, Pd, Ru, and Rh, copper is also a common component in $DeNO_x$ catalysts. Unlike $LaMnO_3$, $LaFeO_3$, $LaCoO_3$, and $LaNiO_3$, the compound $LaCuO_3$ is unstable because it is difficult to keep a high concentration of Cu^{3+} in the bulk of $LaCuO_3$. In the contrary, La_2CuO_4 is very stable [5]. The working oxidation state of copper for the $DeNO_x$ reaction is unclear. For the Cu-ZSM-5 catalysts, Cu^+ was thought to be an active center [6, 7]. London *et al.* suggested that NO decomposition is associated with a redox between Cu^+ and Cu^0 [8]. Mizuno *et al.* reported that Cu^{2+} is an active center for NO

decomposition [9]. The role played by oxygen in the NO decomposition reaction is a topic of controversy [10]. The direct catalytic decomposition of NO to N_2 and O_2 is highly desirable because no additional reactant is needed for the reaction. However, up to now, no suitable material has been obtained to catalyze the reaction under actual exhaust conditions [10-12]. Most of the $DeNO_x$ catalysts are SCR (selective catalytic reduction) catalysts. The substitution of Th^{4+} for La^{3+} in La_2CuO_4 would result in the generation of copper ions of lower oxidation states. Based on such an understanding, we synthesised $La_{1.867}Th_{0.1}CuO_4$ as a catalyst for NO decomposition. According to the $La_{1.867}Th_{0.1}CuO_4$ stoichiometry, 1.65 % of the *A*-site ions are defects. The presence of these *A*-site defects favours the formation of oxygen vacancies. In other words, there are anion vacancies, cationic defects, and copper of lower oxidation states in the $La_{1.867}Th_{0.1}CuO_4$ sample. The activity of the catalyst for NO decomposition has been investigated as related to the intrinsic defect properties of the material.

2. Experimental

2.1 Catalyst preparation

The catalyst was prepared by the citric acid complexing method: lanthanum, thorium, and copper nitrates in a desired molar ratio were dissolved in a citric solution at 80°C with constant stirring until a viscous gel was formed. The gel was decomposed abruptly to very fine powder (ca. 10 nm) at around 300°C. The furnace temperature was then raised (20°C min^{-1}) to 500°C and the catalyst was heated at this temperature in air for 5 h. After being pressed and ground, the catalyst was calcined again at 750°C for 12 h.

2.2 Characterization

The metal-ion composition of the catalyst was determined by titration against standardized solution of EDTA. The oxidation state of copper in the catalyst was measured by means of the iodometry method [13, 14]. Together with the known contents of La^{3+} and Th^{4+}, the data were used to estimate the non-stoichiometric amount of oxygen in the sample.

In situ XRD measurements were carried out on a Rigaku D-Max Rotaflex instrument with Cu$K\alpha$ radiation and Ni filter. The diffraction data were recorded in air as well as in an oxygen atmosphere at temperatures ranging from 20 to 800°C.

BET specific areas were measured on a Nova 1200 instrument. The samples were first treated in a vacuum for 2 h at 400°C before BET measurements.

H_2-TGA was performed on a Rigaku thermoanalyzer. For each measure, 40 mg of fresh (non-reduced) sample was used. A mixture of 10% H_2-90% He (flow rate, 20 mL min^{-1}) was passed through the sample. The temperature range studied was from 20 to 500°C and the heating rate was 10°C min^{-1}.

EPR spectra were recorded at -196°C with a JEOL spectrometer operating in the X-band and calibrated with DPPH (g = 2.004). The sample was placed in a self-made quartz cell in which the sample could be treated under different atmospheres at various temperatures.

For TPD studies, the sample (0.2 g) was placed in the middle of a quartz-reactor (i. d., 4 mm). The outlet gases were analysed on line by mass spectrometry (MS, HP G 1800A). The heating rate was 8°C min^{-1} and the temperature range was from 20 to 800°C. Before performing the O_2-TPD experiment, the sample was heated in O_2 at 300°C for 1h , and then cooled to room temperature in O_2. Before performing the NO-TPD experiment, the sample

was first calcined *in situ* at 800°C for 1 h under a flow of He (20 mL min^{-1}) and then cooled to room temperature. The NO-TPD experiment was performed according to the following procedures: the sample was kept in a flow of NO/He (v/v = 1/100; flow rate, 20 mL min^{-1}) for 1 h at 300°C and then cooled to room temperature. After being He-purged at room temperature for 1 h, the sample was heated to 800°C in helium.

2.3 Catalytic activity measurements

Catalytic activity evaluation was carried out with 0.3 g of sample being packed in a quartz micro-reactor. Prior to the test, the sample was treated at 650°C under a He flow to eliminate water and carbonates. The decomposition of NO was performed between 200 and 800°C (heating rate, 2°C min^{-1}). The reaction feed was 3000 ppm NO in He and the total GHSV was 7500 h^{-1}. Catalytic activity was measured 0.5 h after performance stabilisation. The effluent gases (N_2, NO, and N_2O) were analysed by gas chromatography and mass spectrometry. Before evaluating the catalytic activity of the reduced sample, we carried out the CD_3I-TPD procedure to eliminate surface hydrogen. After three-cycles of CD_3I-TPD treatments, we observed no more CD_3H. It is an indication that most of the surface hydrogen has been eliminated.

3. Results and discussion

3.1 Redox behaviours of catalyst

Based on the data obtained according to the titration methods, the composition of $La_{1.867}Th_{0.1}CuO_4$ is actually $La_{1.867}Th_{0.1}CuO_{4.005}$ whereas that of La_2CuO_4 is $La_2CuO_{4.008}$ (Table 1). The radius of Th^{4+} (0.94 Å) is smaller than that of La^{3+} (1.23 Å). Due to the substitution of Th^{4+} for La^{3+}, the concentration of Cu^{3+} in $La_{1.867}Th_{0.1}CuO_{4.005}$ is lower than that in $La_2CuO_{4.008}$. One can envision that there were cation vacancies and an excess amount of oxygen in $La_{1.867}Th_{0.1}CuO_{4.005}$ ($La_{1.867}Th_{0.1}\phi_{0.033}CuO_{4.005}$, ϕ: cation vacancy).

Figure 1 shows the XRD patterns of fresh $La_{1.867}Th_{0.1}CuO_{4.005}$ and the 100°C-, 300°C-, and 500°C-reduced $La_{1.867}Th_{0.1}CuO_{4.005}$ samples. Fresh $La_{1.867}Th_{0.1}CuO_{4.005}$ is of tetragonal K_2NiF_4-type structure. When it was reduced at 100 and 300°C, respectively, it still retained such a structure. When it was reduced at 500°C, it partially decomposed to $LaCuO_2$, La_2O_3, CuO, and Cu.

Figure 2 shows the TGA profiles of $La_{1.867}Th_{0.1}CuO_{4.005}$. We observed reduction steps at ca. 80, 270, and 420°C. According to the weight losses, the composition of the sample was deduced to be $La_{1.867}Th_{0.1}CuO_{3.996}$, $La_{1.867}Th_{0.1}CuO_{3.977}$, and $La_{1.867}Th_{0.1}CuO_{3.942}$ after the first, second, and third reduction step, respectively. Based on the results of XRD and TGA analyses, we suggest that $La_{1.867}Th_{0.1}CuO_{4-\delta}$ (δ: nonstoichiometric oxygen) decomposed thoroughly when $\delta \geq 0.058$. In $La_{1.867}Th_{0.1}CuO_{3.996}$, almost all the copper ions were Cu^{2+}; in $La_{1.867}Th_{0.1}CuO_{3.977}$, there were 4.7% Cu^+ and 95.3% Cu^{2+}. We deduce that (i) during the first reduction step, Cu^{3+} was reduced to Cu^{2+}; (ii) during the second reduction step, Cu^{2+} was reduced to Cu^+; and (iii) during the third reduction step, the K_2NiF_4-type structure collapsed due to the deep reduction of Cu^+ and the generation of metallic copper.

According to the approach adopted by Wu *et al.* [15]:

$$D = 0.9\lambda/\beta\cos\theta \qquad (1)$$

and

$$\beta^2\cos 2\theta = 4/\pi^2\,(\lambda/D) + 32\,\langle\varepsilon^2\rangle\sin^2\theta \qquad (2)$$

(β: half height width, θ: corresponding Bragg angle, λ = 1.54 Å, D: average thickness of the crystal perpendicular to plane [h k l], $\langle\varepsilon^2\rangle$: square of the average lattice distortion of the polycrystal perpendicular to plane [h k l]),

the average thickness and lattice distortion of the fresh and the 100°C- and 300°C-reduced $La_{1.867}Th_{0.1}CuO_{4.005}$ samples were estimated and the data are listed in Table 2. The lattice parameters a, c, and V are also listed. Based on these data, one can infer that with the rise in reduction temperature, (i) the particle size became smaller; (ii) the extent of lattice distortion increased; and (iii) the lattice prolonged in the c axis and contracted in the a axis. Lattice distortion can be related to the existence of oxygen vacancies: a higher concentration of oxygen vacancies would induce a greater extent of lattice distortion. Being smaller in size and inducing bigger coulombic force, the Th^{4+} ions occupying lattice points of La_2CuO_4 would cause the lattice volume to shrunk.

The EPR spectra of $La_{1.867}Th_{0.1}CuO_{4.005}$ obtained before and after reduction and oxidation are shown in Figure 3. The spectrum of the fresh $La_{1.867}Th_{0.1}CuO_{4.005}$ sample exhibits intensive EPR signals with g = 2.231, 2.130, and 2.059 (Figure 3a); these are typical EPR features of cupric ions [6]. The EPR line is rather broad, possibly due to the high concentration of Cu^{2+}. When the sample was reduced at 100°C, the spectrum intensity decreased dramatically, and a signal with g = 2.007 appeared (Figure 3b). The 2.007 signal is

attributable to electrons trapped at oxygen vacancies [16]. According to the H_2-TGA results, after being reduced at 100°C, the catalyst became $La_{1.867}Th_{0.1}CuO_{3.996}$ and there were oxygen vacancies in the bulk. The reduction would result in Cu^{3+} being converted to Cu^{2+}. After reduction at 300°C, the signal of trapped electrons intensified (Figure 3c). The H_2-TGA result demonstrated that at this stage, more oxygen vacancies were generated and the sample composition was $La_{1.867}Th_{0.1}CuO_{3.977}$. Hence, the reduction process can be described as:

$$Cu^{3+} + e \rightarrow Cu^{2+} \quad (3)$$

$$La_{1.867}Th_{0.1}Cu^{3+}Cu^{2+}O_{4.005} \rightarrow La_{1.867}Th_{0.1}CuO_{4-\lambda} + V_o^{\cdot\cdot} \quad (4)$$

$$e + V_o^{\cdot\cdot} \rightarrow V_e^{\cdot} \quad (5)$$

($V_o^{\cdot\cdot}$ oxygen vacancy, $V_e^{\cdot}$ trapped electron).

When the sample was reduced at 500°C, a signal with g = 2.069 appeared while the signal of trapped electrons weakened (Figure 3d). XRD and H_2-TGA studies revealed that at this stage, the sample had partially decomposed to $LaCuO_2$, La_2O_3, CuO, and Cu. The signal with g = 2.069 represents a kind of cupric ion in new coordination [17]. In other words, there was the generation of a new cupric surface complex. We speculate that the CuO and $LaCuO_2$ phases may be responsible for these new signals. The disappearance of the signal of trapped electron could be due to the demolition of oxygen vacancies due to the collapse of the K_2NiF_4-type structure.

Figure 4 shows the *in situ* XRD patterns during the oxidation of the reduced sample. There were phases of La_2CuO_4, La_2O_3, CuO, and Cu_2O after oxidation at temperatures below 300°C (Figures 4a-c). When the oxidation temperatures were 400 and 500°C, there were

La_2CuO_4, La_2O_3, $LaCuO_2$, and CuO (Figures 4d and 4e). At 600 and 700°C, there was a little amount of La_2O_3 but a large amount of K_2NiF_4-type phase (Figures 4f and 4g). At 800°C, the sample recovered to the former single K_2NiF_4-type structure (Figure 4h). Figures 3e-g show the EPR spectra of a reduced sample being oxidized under an oxygen flow at temperatures between 300 and 800°C. There was no significant change when the oxidation temperature was below 300°C. When the reduced sample was oxidized at 400 and 500°C, signals with g = 2.007, 2.043, and 2.069 could be observed (Figures 3f and 3g). The signals with g values of ca. 2.007 and 2.043 are attributable to O_2^- ions at oxygen vacancies [18-20]. It has been suggested that surface O_2^- species could be formed during thermal treatment *in vacuo* [20]; these oxygen species could enter the oxygen vacancies and participate in the transfer of electrons [19]. The signal with g = 2.069 was due to a new kind of cupric ions at a different coordination environment. This indicates that besides the already existed Cu^{2+} species, there was a new family of cupric ions present at the surface. The XRD patterns indicate that when the oxidation temperatures were between 400 and 500°C, the $LaCuO_2$ and CuO phases appeared. We deduce that the EPR signal with g = 2.069 can be related to these phases. Based on these understandings, we propose the reactions:

$$O_2 + e \rightarrow O_2^- \quad (6)$$

$$Cu_2O + La_2O_3 \rightarrow 2LaCuO_2 \quad (7)$$

$$LaCuO_2 + 1/2La_2O_3 + 1/2O_2^- \rightarrow La_2CuO_4 + 1/2e + V_o^{\cdot\cdot} \quad (8)$$

$$O_2^- + V_o^{\cdot\cdot} \rightarrow O_2^-\text{-}V_o^{\cdot\cdot} \quad (9).$$

At 600 and 700°C, these signals weakened in intensity (Figures 3h and 3i). The XRD patterns showed that at these stages, there was a little amount of $LaCuO_2$ but a large amount of K_2NiF_4-type phase. At 800°C, the EPR spectra recovered to a feature similar to that of a fresh $La_{1.867}Th_{0.1}CuO_{4.005}$ sample (Figure 3j), indicating that the mixtures had recovered to the single K_2NiF_4-type structure.

3.2 The interaction of NO with fresh $La_{1.867}Th_{0.1}CuO_{4.005}$

Figure 5 shows the EPR spectra of NO adsorption on fresh $La_{1.867}Th_{0.1}CuO_{4.005}$ at temperatures ranging from 200 to 800°C. We observed no changes in spectrum features below 400°C (Figures 5a-c), indicating that there was little interaction between NO and the fresh catalyst. At 500°C, there were signals with g = 2.007 and 2.043 (Figure 5d), attributable to O_2^- at oxygen vacancies [18]. At 600 and 700°C, there was a signal with g = 1.987 which can be attributed to NO radicals of low mobility [18]. NO adsorption can generate NO^+, NO^- and $(NO_2)^-$ species [12]. NO^+ is EPR silence. In general, NO^- has been considered as a reaction intermediate for NO decomposition because the bond order of NO^- is 2.0 [21, 22]. As mentioned before, the signals with g = 2.007 and 2.043 are due to O_2^- at oxygen vacancies (Figures 5e and 5f). The formation of N_2O is generally observed in the first stage of NO decomposition [12]. The process can be depicted as:

$$NO + e \rightarrow NO^- \qquad (10)$$

$$4NO^- \rightarrow O_2^- + 2N_2O + 3e \qquad (11).$$

When the sample was exposed to air at room temperature after NO adsorption at 700°C (Figure 5g), the signals with g = 1.987 and 2.043 disappeared, whereas that at 2.007 of trapped electrons diminished in intensity. These indicate that the NO^- and O_2^- species were entirely on the surface; as for the trapped electrons, a small fraction of them was in the bulk.

3.3 NO interaction with $La_{1.867}Th_{0.1}CuO_{4.005}$ pre-reduced at 300°C

Figure 6 shows the EPR spectra of NO adsorption on reduced (at 300°C) $La_{1.867}Th_{0.1}CuO_{4.005}$. We observed that after NO adsorption at 100, 200, and 300°C, there were signals with g = 2.079, 2.043, and 2.028 (Figures 6a-c). The signal with g = 2.079 can be assigned to Cu^{2+} [23]. In other words, NO had oxidized Cu^+ to Cu^{2+}. We deduce that there could be the formation of cupric nitrate. Yasuda *et al.* [24] reported that in La_2CuO_4-based mixed oxides, NO oxidized Cu^{2+} to Cu^{3+}. Munakata *et al.* [25] reported that in $LaBaSrCu_2O_6$, NO adsorption would result in the formation of nitrates. The signal with g = 2.028 can be assigned to the interaction of NO with O_2^- at oxygen vacancies, probably in the form of $[O_2NO_2]^{2-}$ [18]. Again, the signal with g = 2.043 is due to O_2^- at oxygen vacancies. Since we did not observe O_2^- during the thermal treatment of $La_{1.867}Th_{0.1}CuO_{4.005}$, we deduce that besides reactions (10) and (11), there are the following reaction steps:

$$N_2O \rightarrow N_2 + 1/2O_2 \qquad (12)$$

$$NO^- + O_2 \rightarrow NO_3^- \qquad (13)$$

$$NO + 1/2O_2^- \rightarrow NO_2^- \qquad (14)$$

$$NO_2^- + O_2^- \rightarrow [O_2NO_2]^{2-} \quad (15)$$

$$Cu^+ \rightarrow Cu^{2+} + e \quad (16).$$

When we raised the sample temperature to 400°C, there were signals with g = 2.007, 2.028, 2.043, and 2.079 (Figure 6d). The signals at 2.007 and 2.043, 2.028, and 2.079 are due to O_2^- at oxygen vacancies, $[O_2NO_2]^{2-}$, and cupric nitrate, respectively. When the sample temperature was raised to 500 or 600°C, besides the signals observed in Figure 6d, there was a signal with g = 1.987 (Figures 6e, f). The signal with g = 1.987 is due to NO radicals [18]. At 700°C, there were obvious changes in EPR feature (Figure 6g). The signals at 1.987, 2.007, 2.028, and 2.043 still existed, whereas the signal of cupric nitrate vanished. Lin *et al.* reported that nitrate ion was the predominant species at temperatures below 267°C, and its concentration decays at elevated temperatures (> 547°C) [26].

3.4 TPD studies

Figure 7 shows the O_2-TPD curves obtained over the fresh and 300°C-reduced $La_{1.867}Th_{0.1}CuO_{4.005}$ samples. There are two O_2-desorption peaks centered at 370 and 610°C over the fresh sample and three O_2-desorption peaks at ca 260, 370, and 630°C over the reduced one. In general, there are two kinds of O_2-desorption observed on perovskite-type oxides [27]. One is the oxygen (α) at oxygen vacancies and the other is lattice oxygen (β) associated with the redox of *B* ions. There are two α peaks in Figure 7b, implying that compared to the fresh sample, there were more oxygen vacancies in the reduced sample. The

β peak in Figure 7b was bigger than that in Figure 7a, indicating that the lattice oxygen in the reduced sample is more mobile than that in the fresh one.

Figures 8 and 9 are the MS spectra of NO-TPD obtained over the fresh and 300°C-reduced $La_{1.867}Th_{0.1}CuO_{4.005}$ samples, respectively. NO adsorption on the fresh sample produced NO_2 (at ca 80 and 470°C) (Figure 8a), N_2 (at ca 500°C) (Figure 8b), N_2O (at ca 320 and 520°C) (Figure 8c), and NO (at ca 380 and 550°C) (Figure 8d). We did not observe O_2 desorption during the TPD process on a fresh sample. Apparently, there were two different processes for N_2O generation and only one for N_2 production on the fresh sample. As for NO-TPD studies on a reduced sample, we observed O_2 desorption at ca 470°C (Figure 9a), N_2 desorption at ca 470 and 730°C (Figure 9b), N_2O desorption at ca 120, 210, and 470°C, and NO desorption at ca 260 and 460°C. Around 470°C, N_2, O_2, and N_2O were produced; whereas, around 730°C, no O_2 and N_2O were detected. Apparently, there were two different processes for N_2 generation on the reduced sample. We speculate that there are two kinds of intermediates for N_2 generation.

3.5 Catalytic activity

The catalytic activities of NO decomposition at 500°C over the fresh, and 100 °C-, 300 °C-, and 500°C-reduced $La_{1.867}Th_{0.1}CuO_{4.005}$ samples are listed in Table 3. The main products were N_2 and N_2O. The activity of NO decomposition to N_2 is in the order of: 300°C-reduced > 100°C-reduced > fresh > 500°C-reduced $La_{1.867}Th_{0.1}CuO_{4.005}$. The results indicate that a single phase sample of K_2NiF_4-type structure with a high concentration of oxygen vacancies shows the best performance. After reduction at 100 and 300°C, there was the generation of Cu^+ and Cu^{2+}. Reduction at 500°C would result in Cu^0 formation. We suggest that the decomposition

process of NO can be related to a redox action between Cu^{+} and Cu^{2+} in the K_2NiF_4-type lattice.

Figure 10 shows the conversion of NO to N_2 and N_2O as a function of temperature (200 to 800°C) over the fresh and 300°C-reduced $La_{1.867}Th_{0.1}CuO_{4.005}$ catalysts. Within the temperature range, the performance of the reduced sample was better than that of the fresh one. At 650°C, we obtained 91% NO conversion (to N_2) over the former and 35 % NO conversion (to N_2) over the latter; N_2O was a by-product. EPR results demonstrated that NO^{-} was generated on the fresh and reduced samples; NO-TPD studies revealed that N_2O and N_2 were produced simultaneously. We deduce that N_2O and N_2 are produced according to reactions (10) to (12). In EPR studies, we detected the species $[O_2NO_2]^{2-}$ after NO adsorption on a 300°C-reduced $La_{1.867}Th_{0.1}CuO_{4.005}$ sample (Figure 6) but not on a fresh one (Figure 5). We hence deduce that the $[O_2NO_2]^{2-}$ species is responsible for the high activity of NO decomposition over the reduced catalyst. According to the TPD-results of a reduced sample (Figure 9), there was N_2 desorption but no N_2O and O_2 desorption around 750°C. As shown in Figure 7b, there was large desorption of lattice oxygen around 750°C. We deduce that the decomposition of $[O_2NO_2]^{2-}$ could be related to the availability of lattice oxygen. Therefore, we propose that N_2 can also be produced according to the reaction:

$$[O_2NO_2]^{2-} + 6e \rightarrow 4O^{2-} + 1/2N_2 \qquad (17)$$

After the reduction of $La_{1.867}Th_{0.1}CuO_4$, there are plenty of oxygen vacancies in the catalyst and the lattice oxygen becomes more mobile. The former can stabilize O_2^{-} and the latter favour the decomposition of $[O_2NO_2]^{2-}$ to N_2. It has been reported that the addition of a small amount of oxygen could enhance DeNOx activity [28-30]. Valyon and Hall observed that the

oxygen released was different from the oxygen introduced to a Cu-ZSM-5 sample [31]. Based on $^{18}O_2$ and $^{15}NO^{18}$ isotope studies, Valyon *et al.* proposed that an "extra-lattice-oxygen (ELO) species" was involved in NO decomposition [32, 33]. Sachtler and co-workers suggested that ELO is of the form of Cu^{2+}-O^{2-}-Cu^{2+} [34, 35]; whereas Larsen *et al.* suggested that ELO is of the form of $Cu^{2+}O^-$ or $Cu^{2+}O_2^-$ [36]. Iwamoto *et al.* reported that at high temperatures, oxygen desorption can regenerate the active sites and thus make it possible to continue the catalytic cycle for NO decomposition [22]. Lin *et al.* suggested that NO_2 species can be generated by the interaction between NO and oxygen atom over $YBa_2Cu_3O_7$ [26]. We envision that the redox action between O_2^- and O^{2-} (Cu^+-O_2^-- Cu^{2+}-O^{2-}) is involved in the decomposition of NO over $La_{1.867}Th_{0.1}CuO_4$.

4. Conclusion

When $La_{1.867}Th_{0.1}CuO_4$ was reduced at temperatures between 100 and 300°C, it retained a single phase of K_2NiF_4-type structure, with oxygen vacancies and trapped electrons being created in the lattice. The K_2NiF_4-type structure collapsed at 500°C to a mixture of oxides. Such a mixture could be oxidized at 800°C to the former single phase. During the oxidation process, O_2^- species was generated at oxygen vacancies. The $La_{1.867}Th_{0.1}CuO_4$ sample reduced at 300°C showed a high concentration of oxygen vacancies and the Cu^+ ions in it exhibited better NO decomposition activity than those in the fresh and 100°C-reduced samples. During NO adsorption, NO^- was generated on both fresh and 300°C-reduced samples, whereas $[O_2NO_2]^{2-}$ was only detected on the reduced sample. We propose that $[O_2NO_2]^{2-}$ is a key intermediate for N_2 production. Oxygen vacancies can stabilise O_2^- species and a high mobility of lattice oxygen favours the decomposition of $[O_2NO_2]^{2-}$. The redox

between Cu^{2+} and Cu^{+} as well as that between O_2^- and O^{2-} might be involved in the decomposition of NO over the reduced catalyst.

Acknowledgement

The work described above was fully supported by a grant from the Hong Kong Baptist University (FRG/97-98/I-30).

References

[1] K. Tabata and M. Misono, Catal. Today 8 (1990) 249.

[2] Z.L. Yu, L.Z. Gao, S.Y. Yuan, and Y. Wu, J. Chem. Soc. Faraday Trans. 88 (1992) 3245.

[3] S.D. Peter, E. Garbowski, N. Guilhaume, V. Perrichon, and M. Primet, Catal. Lett. 54 (1998) 79.

[4] L.Z. Gao, Z.L. Yu, and Y. Wu, *Proc. 34th IUPAC Congr.* P. 730.

[5] L.Z. Gao, Z.L. Yu, and Y. Wu, Acta Chimica Sinica 55 (1997) 56.

[6] M. Anpo, M. Matsuoka, Y. Shioya, H. Yamashita, E. Giamello, C. Morterra, M. Che, H.H. Paterson, S. Webber, S. Oullete, and M.A. Fox, J. Phys. Chem. 98 (1994) 5744.

[7] E. Giamello, D. Murphy, G. Magacca, C. Morterra, Y. Shioya, T. Nomura, and M. Anpo, J. Catal. 136 (1992) 510.

[8] J.W. London and A.T. Bell, J. Catal. 31 (1973) 96.

[9] N. Mizuno, M. Yamato, and M. Tanaka, Chem. Material 1 (1989) 232.

[10] G.J. Millar, A. Canning, G. Rose, B. Wood, L. Trewartha, and I.D.R. Mackinnon, J. Catal. 183 (1999) 169.

[11] E.S.J. Lox and B.H. Engler, *Handbook of Heterogeneous Catalysis Vol. 4* (Eds: G. Ertl, H. Knözinger, and J. Weitkamp), p. 1628.

[12] V.I. Pârvulescu, P. Grange, and B. Delmon, Catal. Today 46 (1998) 233.

[13] L.K.Gushee and R. Ward, J. Am. Chem. Soc. 79 (1957) 5601.

[14] D.C. Harris and T.A. Hewton, J. Solid State Chem. 69 (1987) 182.

[15] Y. Wu, B.S. Dou, C.X. Wang, X.F. Xie, Z.L. Yu, S.R. Fan, and L.C. Wang, J. Catal. 120 (1989) 88.

[16] C.T. Au and X.P.Zhou, J. Chem. Soc., Faraday Trans. 92 (1996) 1793.

[17] C. Morterra, E. Giamello, G. Gerrato, G. Centi, and S. Perathoner, J. Catal. 179 (1989) 111.

[18] A. Martínez-Arias, J. Sorria, J.C. Conesa, X.L. Seoane, A. Arcoya, and R. Cataluña, J. Chem. Soc. Faraday Trans. 91 (1995) 1679.

[19] C. Oliva, L. Forni, A.M. Ezerets, I.E. Mukovozov, and A.V. Vishniakov, J. Chem. Soc. Faraday Trans. 94 (1998) 587.

[20] Z. X. Zhang and K.J. Klabunde, Inorg. Chem., 31 (1992) 1706.

[21] Z Zhao, X.G. Yang, and Y. Wu, Science in China B 28 (1998) 31.

[22] M. Iwamoto, H. Furukawa, and S. Kagawa, in : New Developments in Zeolite Science and Technology, Studies in surface Science and Catalysis, vol. 28, (Eds: Y. Murakami, A. Iijima, and J.W. Ward), Elsevier, Amsterdam, 1986, P. 943.

[23] Z. Sojka, M. Che, and E. Giamello, J. Phys. Chem. B. 101 (1997) 4831.

[24] H. Yasuda, T. Nitadori, N. Mizuno, and M. Misono, Bull. Chem. Soc. Jpn. 66 (1993) 3492.

[25] F. Munakata, Y. Akimune, Y. Shichi, M. Akutsu, H. Yamaguchi, and Y. Inoue, Chem. Commu. (1997) 63.

[26] J.Y. Lin, A.T.S. Wee, K.L. Tan, K.G. Neoh, and W.K. Teo, Inorg. Chem. 32 (1993) 5322.

[27] H.X. Dai, C.F. Ng, and C.T. Au, Catal. Lett. 57 (1999) 115.

[28] Z. Chajar, M. Primet, and H. Praliaud, J. Catal. 180 (1998) 279.

[29] M. Shelf, Chem. Rev. 95 (1995) 209.

[30] Y.F. Chang and J.G. McCarty, J. Catal. 178 (1998) 408.

[31] J. Valyon and W.K. Hall, Catal. Lett. 19 (1993) 109.

[32] J. Valyon and W.K. Hall, J. Catal. 143 (1993) 520.

[33] J. Valyon, W.S. Millman, and W.K. Hall, Catal. Lett. 24 (194) 215.

[34] J. Sarkany, J.L. D'Itri, and W.M.H. Sachtler, Catal. Lett. 16 (1992) 241.

[35] G.D. Lei, B. J. Adelman, J. Sarkany, and W.M.H. Sachtler, Appl. Catal. B 5 (1995) 245.

[36] S.C. Larsen, A.W. Aylor, A.T. Bell, and J.A. Reimer, J. Phys. Chem. 98 (1994) 11533.

Captions

Figure 1. *In situ* XRD patterns of (a) fresh, (b) 100°C-, (c) 300°C-, and (d) 500°C-reduced $La_{1.867}Th_{0.1}CuO_4$.

Figure 2. TGA curves of $La_{1.867}Th_{0.1}CuO_4$.

Figure 3. EPR spectra of (a) fresh, (b) 100°C-, (c) 300°C-, and (d) 500°C-reduced $La_{1.867}Th_{0.1}CuO_4$; then after oxidation at (e) 200°C, (f) 300°C, (g) 400°C, (h) 500°C, (i) 600°C, and (j) 700°C.

Figure 4. *In situ* XRD patterns of a 500°C-reduced $La_{1.867}Th_{0.1}CuO_4$ sample oxidized at (a) 100°C, (b) 200°C, (c) 300°C, (d) 400°C, (e) 500°C, (f) 600°C, (g) 700°C, and (h) 800°C.

Figure 5. EPR spectra of NO adsorption on fresh $La_{1.867}Th_{0.1}CuO_4$ at (a) 200°C, (b) 300°C, (c) 400°C, (d) 500°C, (e) 600°C, and (f) 700°C; and (g) the sample was exposed to air at room temperature.

Figure 6. EPR spectra of NO adsorption on a 300°C-reduced $La_{1.867}Th_{0.1}CuO_4$ sample at (a) 100°C, (b) 200°C, (c) 300°C, (d) 400°C, (e) 500°C, (f) 600°C, and (g) 700°C.

Figure 7. O_2-TPD profiles obtained over (a) a fresh and (b) a 300°C-reduced $La_{1.867}Th_{0.1}CuO_4$ sample.

Figure 8. NO-TPD profiles obtained over a fresh $La_{1.867}Th_{0.1}CuO_4$ sample. (a) NO_2, (b) N_2, (c) N_2O, and (d) NO.

Figure 9. NO-TPD profiles obtained over a 300°C-reduced $La_{1.867}Th_{0.1}CuO_4$ sample. (a) O_2, (b) N_2, (c) N_2O, and (d) NO.

Figure 10. NO conversion to N_2 (hollow) and N_2O (solid) versus reaction temperature over fresh (square) and 300°C-reduced (triangle) $La_{1.867}Th_{0.1}CuO_4$.

Table 1

Cu^{3+} concentrations, surface areas, and compositions of La_2CuO_4 and $La_{1.867}Th_{0.1}CuO_4$

Samples	Cu^{3+}/Cu (%)	Surface (m^2/g)	Composition
La_2CuO_4	1.5	2.8	$La_2CuO_{4.008}$
$La_{1.867}Th_{0.1}CuO_4$	1.0	3.5	$La_{1.867}Th_{0.1}CuO_{4.005}$

Table 2

D_{110}, $\langle\varepsilon^2\rangle^{1/2}$, a, c, and V values of fresh, and 100°C- and 300°C-reduced $La_{1.867}Th_{0.1}CuO_{4.005}$ samples

Samples	D_{110} (nm)	$\langle\varepsilon^2\rangle_{110}^{1/2}$ (10^{-3})	a (nm)	c (nm)	V (nm^3)
Fresh	20.15	2.83	0.5353	1.3213	0.3786
reduced at 100°C	20.70	2.97	0.5335	1.3248	0.3771
reduced at 300°C	19.72	3.12	0.5328	1.3261	0.3764

Table 3

Catalytic activities at 500°C of fresh, and 100°C- and 300°C-reduced $La_{1.867}Th_{0.1}CuO_{4.005}$ samples

Reduction temp. (°C)	Fresh	100	300	500
NO conversion to N_2 (%)	26	40	65	25
NO conversion to N_2O (%)	21	12	7	7

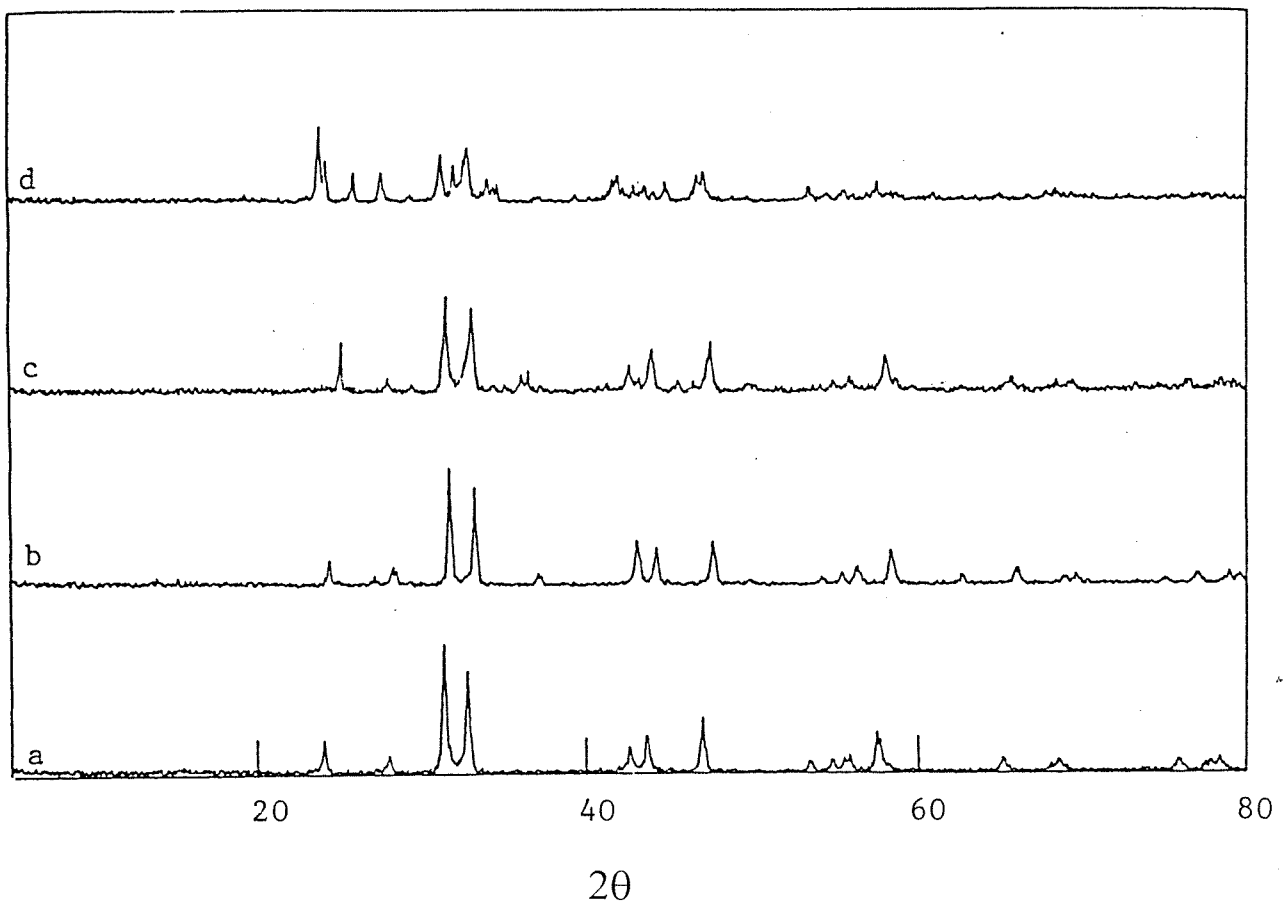

Figure 1. *In situ* XRD patterns of (a) fresh, (b) 100°C-, (c) 300°C-, and (d) 500°C-reduced $La_{1.867}Th_{0.1}CuO_4$.

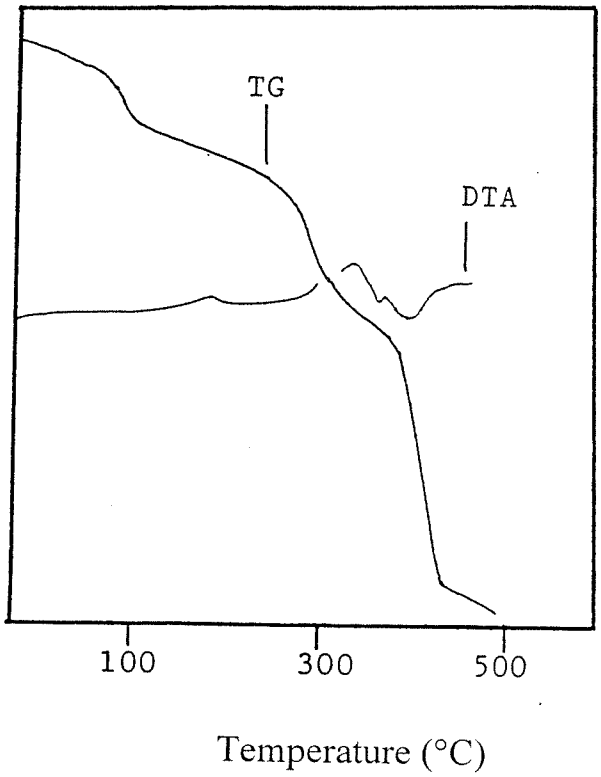

Figure 2. TGA curves of $La_{1.867}Th_{0.1}CuO_4$.

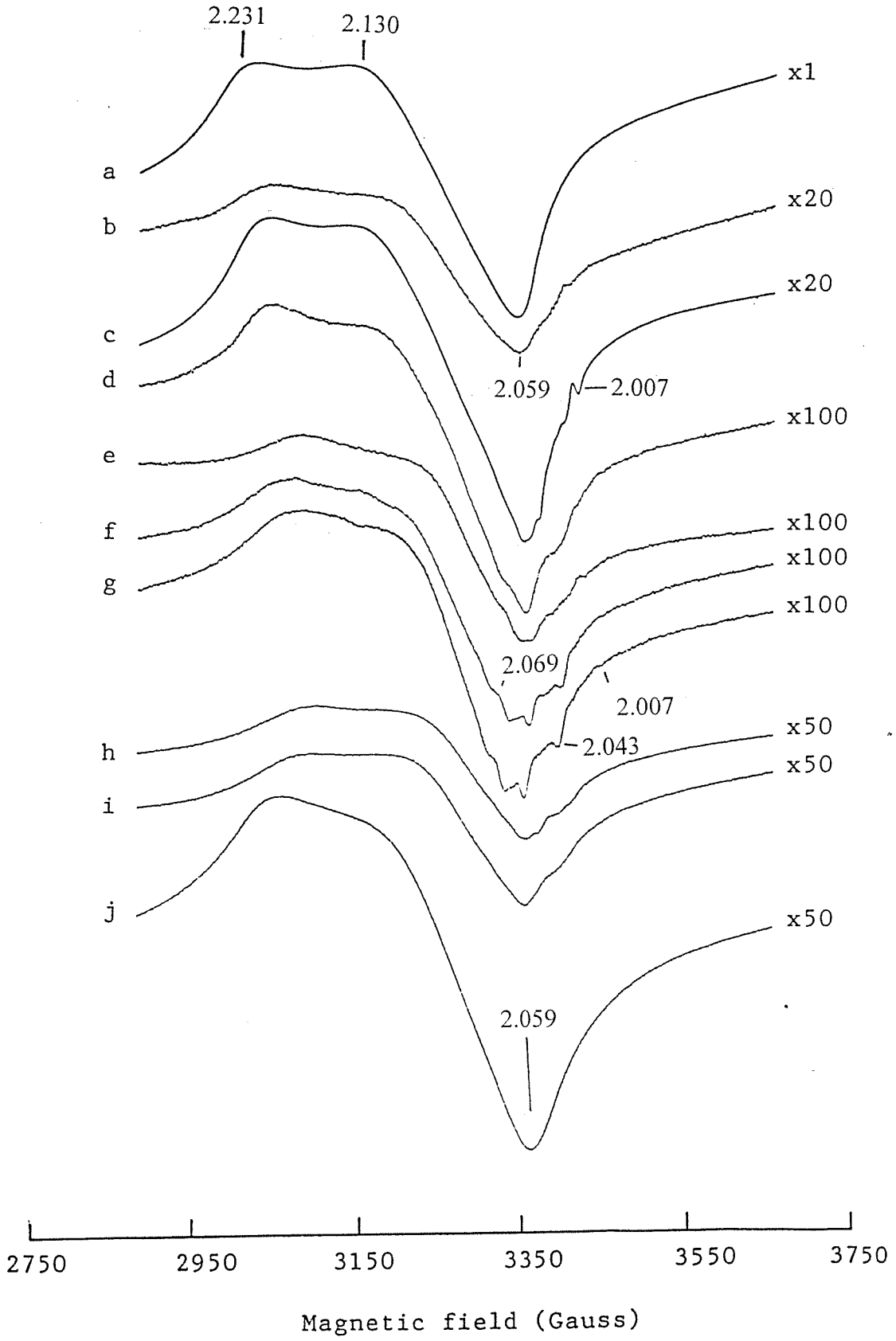

Figure 3. EPR spectra of (a) fresh, (b) 100°C-, (c) 300°C-, and (d) 500°C-reduced $La_{1.867}Th_{0.1}CuO_4$; then after oxidation at (e) 200°C, (f) 300°C, (g) 400°C, (h) 500°C, (i) 600°C, and (j) 700°C.

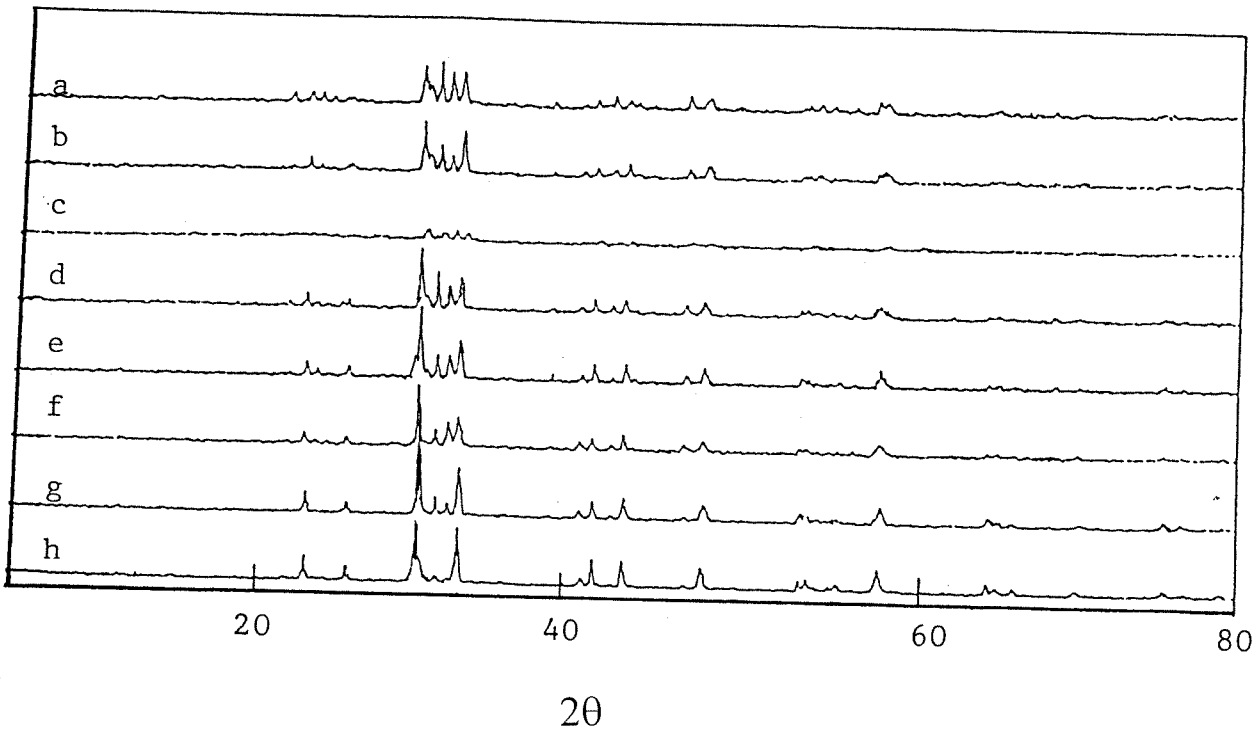

Figure 4. *In situ* XRD patterns of a 500°C-reduced $La_{1.867}Th_{0.1}CuO_4$ sample oxidized at (a) 100°C, (b) 200°C, (c) 300°C, (d) 400°C, (e) 500°C, (f) 600°C, (g) 700°C, and (h) 800°C.

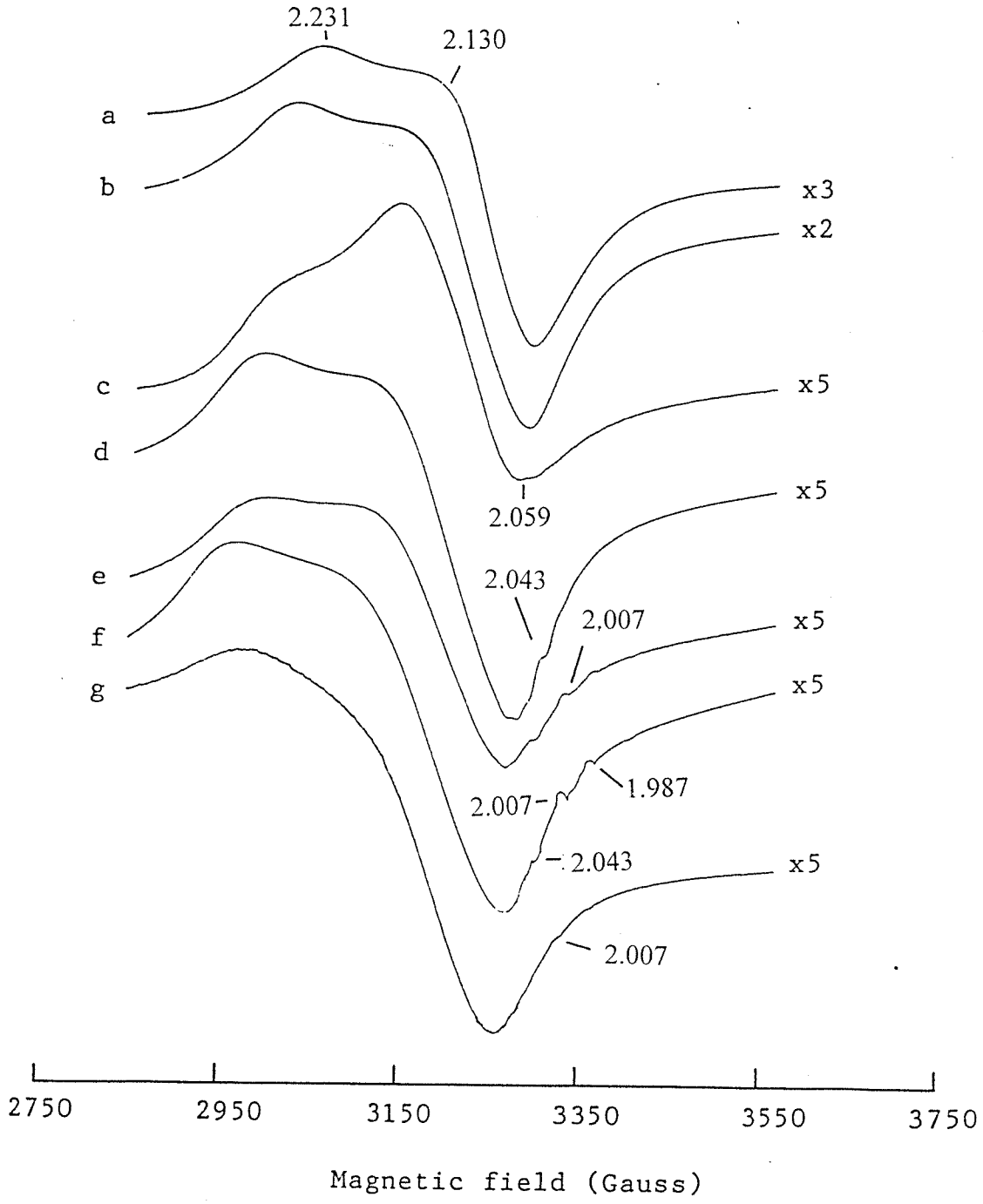

Figure 5. EPR spectra of NO adsorption on fresh $La_{1.867}Th_{0.1}CuO_4$ at (a) 200°C, (b) 300°C, (c) 400°C, (d) 500°C, (e) 600°C, and (f) 700°C; and (g) the sample was exposed to air at room temperature.

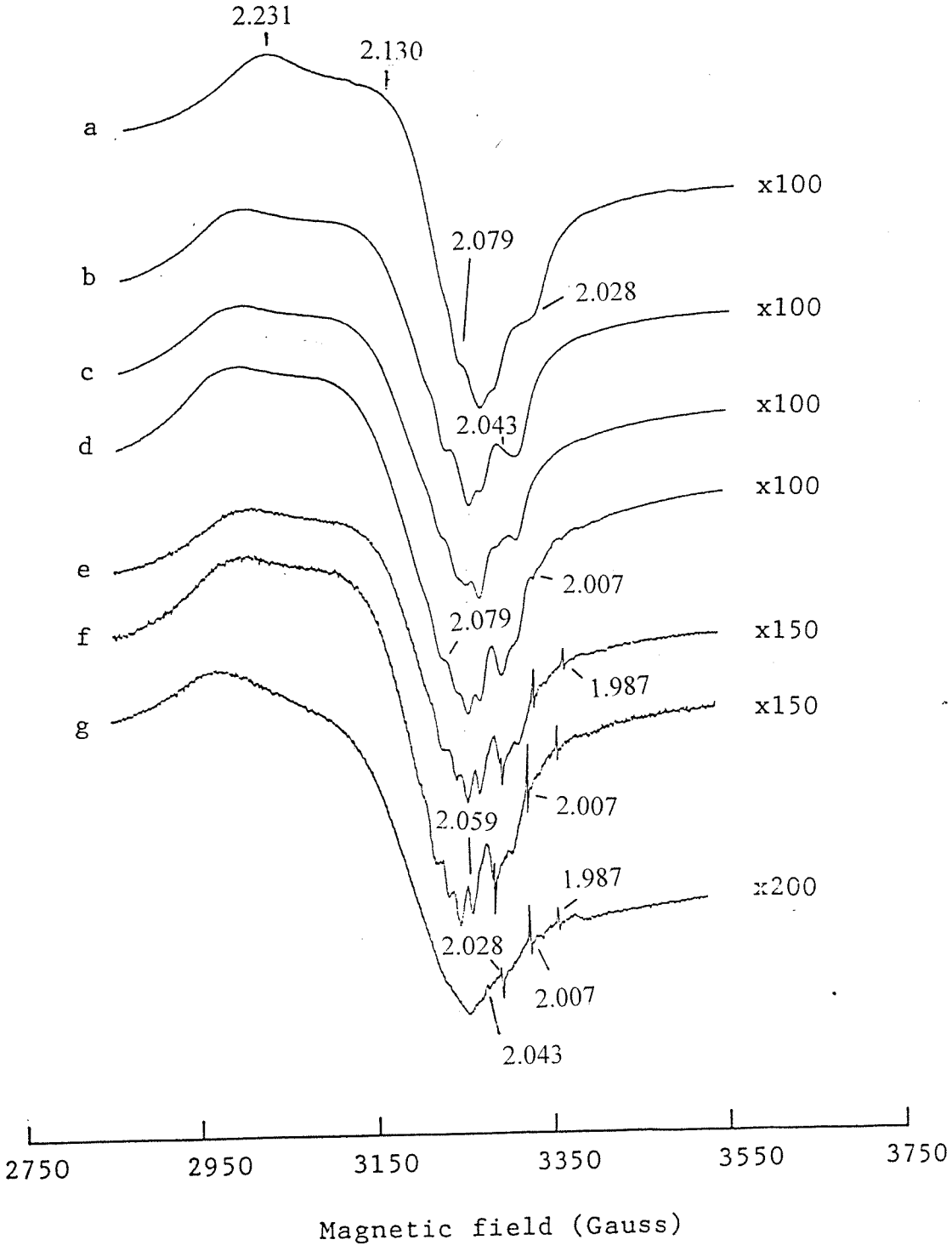

Figure 6. EPR spectra of NO adsorption on a 300°C-reduced $La_{1.867}Th_{0.1}CuO_4$ sample at (a) 100°C, (b) 200°C, (c) 300°C, (d) 400°C, (e) 500°C, (f) 600°C, and (g) 700°C.

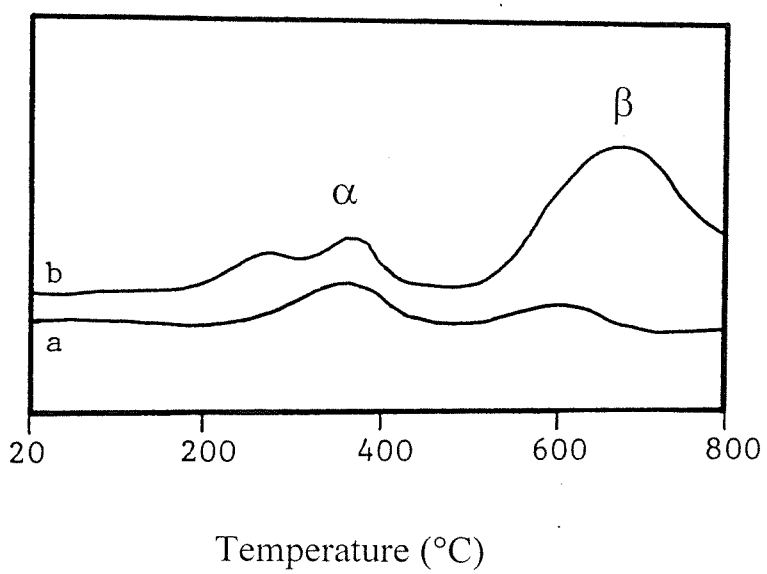

Figure 7. O_2-TPD profiles obtained over (a) a fresh and (b) a 300°C-reduced $La_{1.867}Th_{0.1}CuO_4$ sample.

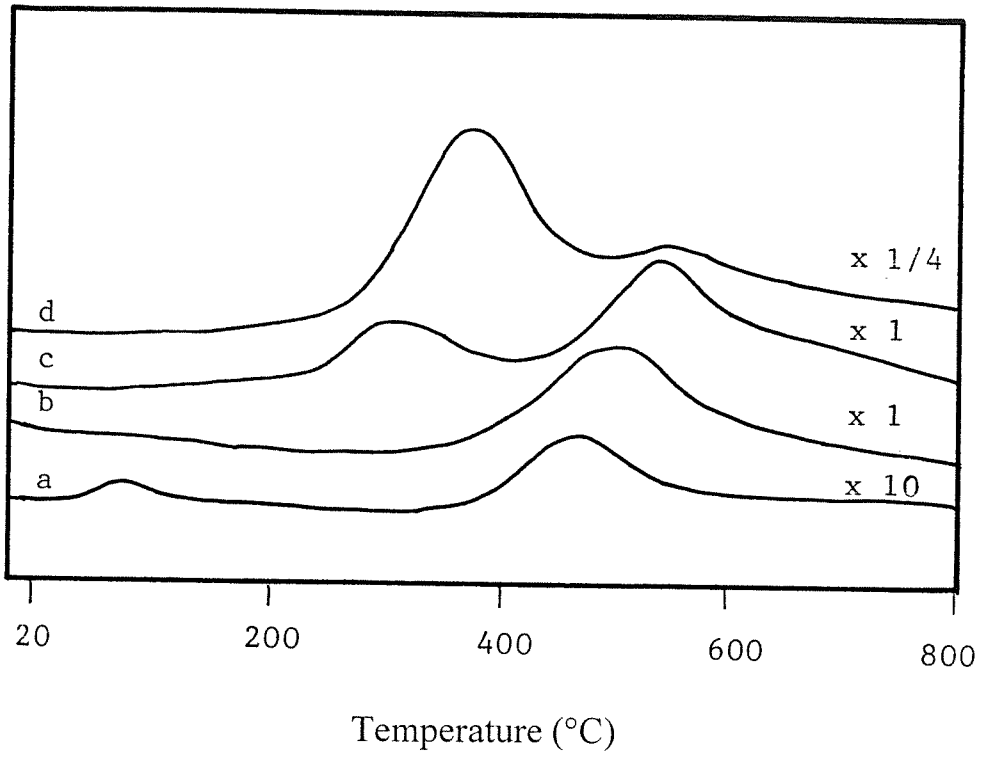

Figure 8. NO-TPD profiles obtained over a fresh $La_{1.867}Th_{0.1}CuO_4$ sample. (a) NO_2, (b) N_2, (c) N_2O, and (d) NO.

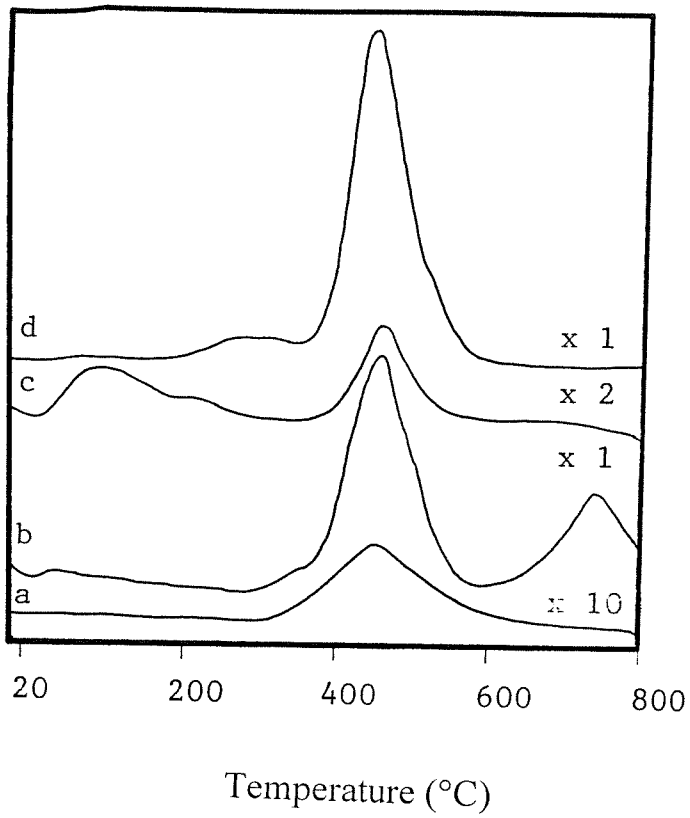

Figure 9. NO-TPD profiles obtained over a 300°C-reduced $La_{1.867}Th_{0.1}CuO_4$ sample. (a) O_2, (b) N_2, (c) N_2O, and (d) NO.

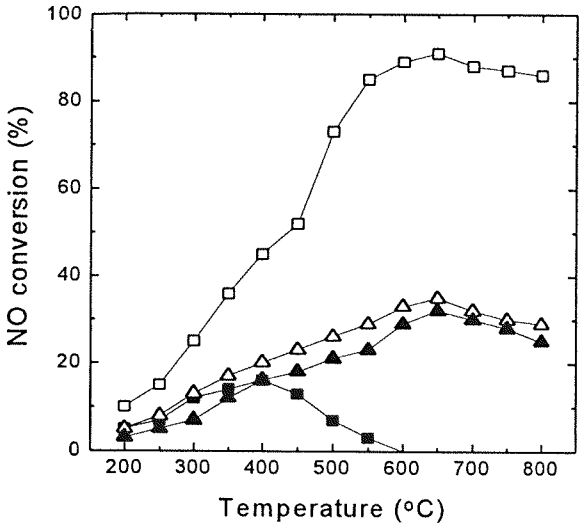

Figure 10. NO conversion to N_2 (hollow) and N_2O (solid) versus reaction temperature over fresh (square) and 300°C-reduced (triangle) $La_{1.867}Th_{0.1}CuO_4$.